Hongan LI[1], Yuyou YANG[1], Xiaoming TU[1], Ting WANG[2]

China University of Geosciences (Beijing) (1), Beijing Municipal Engineering Group Co.,Ltd (2)

Analysis of jacking force for rectangular pipe-jacking machine

Abstract. For the electrical control system of push pipe driving machine, the adjustment of jacking force is critical to balancing the resistance force and moving the pipe string forward. This force should be well under control so as to avoid both the collapse (active failure) and the blow-out (passive failure) of the soil mass near the tunnel face. The aim of this paper is to determine the collapse and blow-out face jacking force of a rectangular tunnel. The analysis is carried out in the framework of the kinematic method of limit analysis theory. The numerical results obtained are presented and analyzed.

Streszczenie. W maszynach do przeciskania rur istotną role odgrywa siła przecisku (jacking force). W artykule analizuje się tę siłę dla prostokątnego tunelu. (Analiza siły przecisku w przypadku drążenia tunelu prostokątnego przez maszynę przeciskającą rurę).

Keywords: Jacking force, Rectangular pipe-jacking machine, Limit analysis.
Słowa kluczowe: siła przecisku, drążenie tunelu

1. Introduction

Pipe-jacking is a technique employed for installing an underground pipe using a shield type driven machine. Compared with the traditional trench excavating method, this technique possesses the rapid, secure and efficient construction and has tiny impact on the environment and the traffic of the construction area. Pipe-jacking is widely used in recent years around the world. The face stability is a key point in construction of underground tunnels. To guarantee tunnel face safety, the determination of the jacking force applied to the face by the shield is required. A soil collapse failure will occur when the jacking force is not enough to prevent the movement of the soil mass towards the tunnel. On the other hand, a blow-out failure appears when the jacking force is so great that soil is heaved in front of the shield. The aim of the face stability analysis is to ensure safety against soil collapse and blow-out in front of the tunnel face. In the construction process, jacking force is setting mostly on the basis of the experience of operator. And the adjustment of jacking force mainly relies on the artificial control method, which leads to some engineering accidents, such as ground settlement, ground uplift, difficultly in pushing the pipe and collapse failure and so on. With the development of electronic technology, the automated control system that integrates computer technique with photoelectric measuring system and remote control system is generated and more usually used in real-time monitor and adjustment of jacking force. Although this method can reduce the engineering accidents to a certain extent, the determination of jacking force needs to be perfected in terms of theory.

The study of the analysis of jacking force has been investigated by several authors in the literature. D.N. Chapman and Y. Ichioka proposed equations for estimating the jacking forces associated with different types of microtunnelling operations and soil [1]. K.J. Shou and F.W. Chang analysed the soil behaviour during pipe-jacking by means of physical and numerical models. Their study proved that the improper control of jacking force may cause the collapse failure or blow-out failure, and a characteristic curve was given [2]. Marco Barla *et al.* studied the jacking force on the basis of a field case, the results of which showed that there were two sloping sections for each drive. And the second part needed to take account of the increased friction due to the bore instability [3]. All these studies focus on the regular circular tunnels, and predict that the jacking force depends on experience, field cases or numerical methods. Due to recent advances and innovations in theory and practice, the constructions of non-circular cross section tunnels come true. However, in fact,

traditional studies concentrate mainly on circular tunnels and many theories about the non-circular tunnels are incomplete. As establishing a 3D failure model is extremely challenging, few efforts have been made to carry out such research. This paper focuses on the analysis of face stability of a rectangular tunnel for pipe-jacking. The attempt of obtaining the bound of jacking force may be realized by means of the kinematical approach of the limit analysis theory. Two 3D numerical mechanisms associated with the rectangular tunnels are proposed in this paper. Then, the numerical results of both the failure mechanisms are presented and analyzed. The results in the paper may serve as practical tools for face stability assessment of rectangular tunnels.

2. Kinematical method of limit analysis

The aim of the stability analysis is to ensure safety against soil failure in front of the tunnel face. Stability conditions for this system are derived in terms of the loads that can be applied to the system without causing failure. An upper bound estimation of such loads is obtained by considering a kinematically admissible failure mechanism for which the power of the loads applied to the system is larger than the power that can be dissipated inside the system during its movement (the upper bound theorem) [4]. Limit analysis was presented in terms of the theorems by Drucker *et al.* [5] to estimate the critical height of slope. In fact, the problem of tunnel face stability is a typical problem where a boundary limit load is sought, so the limit analysis method is perfectly suited. The kinematical theorem in limit analysis is based on the work equation which states that the rate of work done by external and body forces is less than or equal to the rate of internal energy dissipation for a kinematically admissible velocity field with respect to the flow rule and the velocity boundary conditions. Generally it can be described in the following mathematical form:

$$(1) \quad \int_V D(\dot{\varepsilon}_{ij})dV \geq \int_{S_v} T_i v_i dS_v + \int_{S_t} T_i v_i dS_t + \int_V \gamma_i v_i dV$$

The left side of Eq. (1) represents the rate of work dissipation during an incipient failure of a structure, and the right side includes the work rates of all external forces. T_i is the stress vector on boundaries S_v and S_t. Vector T_i is unknown (limit load) on S_v, yet known on S_t (for instance, surcharge pressure). v_i is the velocity vector in the kinematically admissible mechanism, γ_i is the specific weight vector, and V is the volume of the mechanism [6].

In this paper, the soils satisfy the Mohr–Coulomb yield condition, and an associated flow rule is adopted. The

Mohr–Coulomb function contains two material constants: the internal friction angle φ and the cohesion intercept c. For purely frictional material $c=0$, while for purely cohesive soil $\varphi=0$, with the cohesion identified with undrained strength ($c=c_u$). In the case of a three-dimensional and continuous deformation field, the flow rule requires the following relationship among the principal strain rates:

$$(2) \quad \dot{\varepsilon}_1 + \dot{\varepsilon}_2 + \dot{\varepsilon}_3 + (\dot{\varepsilon}_1 - \dot{\varepsilon}_2 - \dot{\varepsilon}_3)\sin\varphi = 0$$

The solutions will be obtained by simplifying two conditions: the plane strain-type ($\dot{\varepsilon}=0$) with the material is purely cohesive ($\varphi=0$) and the failure mechanism is of the rigid-block motion type. In the last case, strain rates are zero within the rigid blocks, and Eq. (2) is satisfied within blocks identically. The blocks are separated by velocity discontinuity surfaces, where the velocity jump vectors must be inclined at angle $\varphi=0$ to the discontinuities: that is

$$(3) \quad [v_n] = [v_t]\tan\varphi$$

where: $[v_n]$ and $[v_t]$ are the normal and tangential components of the velocity jump vector $[v_i]$ respectively [10].

3. Collapse failure
3.1 Geometrical construction of the 3D collapse failure surface

It is not common to construct a 3D failure mechanism of a shallow tunnel with a rectangular cross section driven by the pressurized shield. Traditional studies focused on the single circle tunnels. Some failure mechanisms were proposed by some authors to estimate the limit pressures applied to the tunnel face. Leca and Dormieux [4] proposed a mechanism composed of two conical blocks for the collapse case and a mechanism composed of a single conical block outcropping at the ground surface for the blow-out case. A.-H. Soubra and D. Dias *et al.* [8] improved the mechanism by considering a new mechanism consisting of more rigid truncate cones, and presented more optimized results. It is necessary to state that the study in this paper is inspired by the achievements mentioned above.
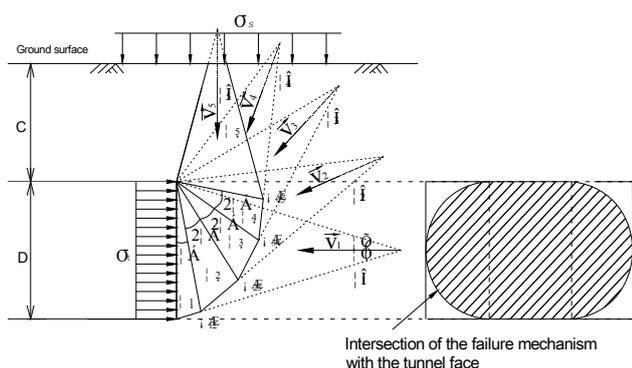

Fig.1. Collapse mechanism (M1)

At first, the 3D failure surface of a regular tunnel with a circular cross section is considered. This mechanism is of multi-blocks. It involves the movement of n truncated solid conical blocks with circular cross-sections. The opening of each cone is equal to 2φ and its velocity is parallel to its axis. A mechanism with $n=5$ is presented in Fig. 1. Note that ξ_i (i=1, 2, 3…n) denotes the cone, and Ω_i (i=1, 2, 3…n) denotes the truncated block. The presented mechanism is completely defined by the angular parameter α, and the

blocks number n. Then, based on the study of the single-circular tunnel, the mechanism can be modified with cylindrical inserts, to ensure transition to a plane mechanism with an increase in the width of the insert [9]. The tunnel face can be idealized as a combination assembly by two semi-circles with diameter D and a rectangle with width D as shown in Fig. 1. Notice finally that whether the upper rigid cone ξ_n in the mechanism will or will not intersect the ground surface depends on the φ and C/D values.
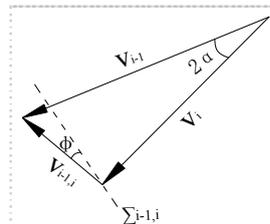
3.2 Velocity field

Fig.2. Velocity hodograph between two successive blocks

The collapse failure mechanism is a translational kinematically admissible failure mechanism. The different blocks of this mechanism move as rigid bodies. The velocity vector of each block has different directions and magnitude. According to the normality condition for an associated flow rule Coulomb material, for a kinematically admissible failure mechanism, the velocity discontinuity along a plastically deformed surface must make an angle φ with this velocity discontinuity surface [10]. The velocity hodograph is given in Fig. 2, where, i=1, 2,…, n, n is the number of blocks; parameter α is the angle between the contact surface and the vertical direction.

3.3 Work equation

For a kinematically admissible velocity field the bound on the limit supporting force is determined by equating the rate of work of external forces W to the rate of work D. This is often referred to as the energy rate balance. In this paper, the external forces contributing to the rate of external work consist of (i) the self-weight of the soil (ii) the possible surcharge loading σ_s and (iii) the pressure σ_t acting on the face of the tunnel. Hence, the unknown limit load (iii) can be calculated by using Eq. (1). Associated with the face stability analysis of tunnels driven by the pressurized shield, Eq. (1) is transformed to the following form:

$$(4) \quad D = W_\gamma + W_S + W_T$$

where: D represents the rate of dissipation energy, and W_γ, W_S, W_T represents the rate of work done by self-weight, surcharge load, and jacking force respectively.

By means of the velocity transformation relationship mentioned above, the calculations concerning the rate of work of these forces were carried out.

Rate of work of the soil weight is calculated from a general expression as Eq. (5).

$$(5) \quad W_\gamma = \iiint_V v_i \gamma_i dV = \gamma v \sin\beta V$$

where: v_i and γ_i—velocity vector and the unit weight vector, respectively, and v and γ—magnitudes, V—the volume of the mechanism (underground surface).

Rate of work of the possible uniform surcharge σ_s acting on the ground surface is calculated from a general expression as Eq. (6).

(6)
$$W_S = \sigma_S \iint_S v_i dS = \sigma_S v \sin \beta A_2$$

where: A_2—the possible area of the intersection of the mechanism with ground surface.

Rate of work of the pressure σ_t is calculated from a general expression as Eq. (7).

(7)
$$W_T = -\sigma_t \iint_S v_i dS = -\sigma_t v \cos \beta A_1$$

where: A_1—the area of intersection of the tunnel face with the lower cone.

Considering that the mechanism is rigid, the source of energy dissipation derived from the plastic soil deformation only occurs along the velocity discontinuity surface. Rate of internal energy dissipation is calculated from a general expression as Eq. (8).

(8)
$$D = \iint_S c v_i \cos \varphi dS = c v \cos \varphi S$$

where: S—the superficial area of the mechanism (underground surface).

It should be mentioned here that the computation of energy dissipation could also be made by using an alternative convenient approach (for more details, see Michalowski and Drescher [7]).

By equating the total rate of external forces (Eq. (5)-(7)) to the total rate of internal energy dissipation (Eq. (8)), the pressure σ_t can be expressed as follows:

(9)
$$\sigma_t = \gamma D N_\gamma + \sigma_S N_S + c N_c$$

where: N_γ, N_c and N_s are non-dimensional coefficients, representing respectively the effect of soil self-weight, cohesion and surcharge loading.

Notice that N_c and N_s are related by the following classical formula (see theorem of corresponding states):

(10)
$$N_c \tan \varphi + 1 - N_s = 0$$

Hence, in the following, only coefficients N_γ and N_s will be presented, coefficient N_c can be obtained through Eq. (10).

3.4 Numerical results of M1 (collapse)

In this section, the values of parameter N_γ^c, N_s^c and the critical failure pressure σ_c for M1 are presented. From Fig. 3, it is obvious that, for the same φ, N_γ^c increases with C/D; for the same C/D, N_γ^c decreases as φ increases. However, N_s^c decreases with the increase of C/D value and vanishes beyond a certain C/D, which corresponding to the condition of no-outcrop of the upper block. In this case, the surcharge loading σ_s will have no influence on the critical N_s^c value. Then, for higher values of φ, it becomes constant for the large C/D values corresponding to the condition of no-outcrop of the upper cone. The phenomenon becomes inconspicuous for lower values of φ because it becomes harder for the mechanism to outcrop the ground with the decrease of φ. The same phenomenon appears in the charts of N_s^c. These conclusions coincide with those of Leca and Dormieux [4].

It is necessary to mention that the number of blocks influences the results of N_γ^c, N_c^c and N_s^c. After a detailed calculation, the results show that with the increasing of n, the results tend to be more optimized. However, when $n>10$, the improvement percentage is smaller than 1%. Hence, the results presented in this paper are related to $n=10$.

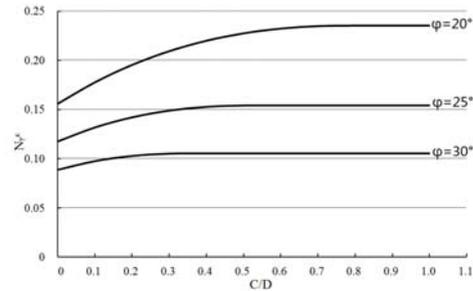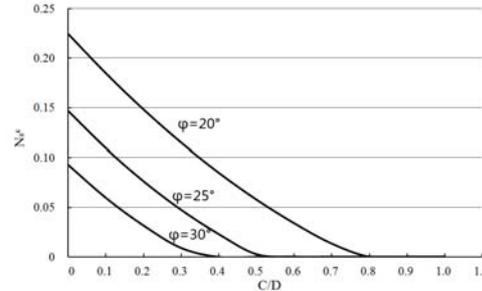Fig.3. Values of N_γ^c

Fig.4. Values of N_s^c

Through a series of analysis, a characteristic curve for the limit jacking force σ_c is drawn as shown in Fig. 5. This curve reveals a lower bound, below which collapse failure will occur. When the value of C/D is small, the upper block is outcrop, σ_c decreases with the increasing of C/D; the curve becomes constant for the large values of C/D corresponding to the condition of no-outcrop of the upper block. The trend is consistent with the actual situation. It is necessary to note that the case of the $C/D<0.5$ is impractical, so the curve of the limit jacking force does not start from $C/D=0$.
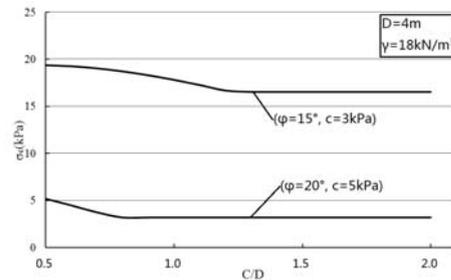

Fig.5. Critical collapse failure pressure σ_c

4. Blow-out failure
4.1 Geometrical construction of the 3D blow-out failure surface

The blow-out failure will occur when the jacking force is so large that soil is heaved in front of the shield. As shown in Fig. 6, M2 is a blow-out mechanism. Only two blocks are necessary for the blow-out mechanism since an increase in the number of blocks improves the solutions by only a few percent (1%). The geometrical construction of M2 is similar to that of M1, while the M2 mechanism presents an upward movement of the soil mass in front of the shield. Thus, the cones with an opening angle 2φ are reversed. And contrary to M1, M2 is always outcrops. The mechanism is also modified with cylindrical inserts, to ensure transition to a plane mechanism with an increase in the width of the insert [9].
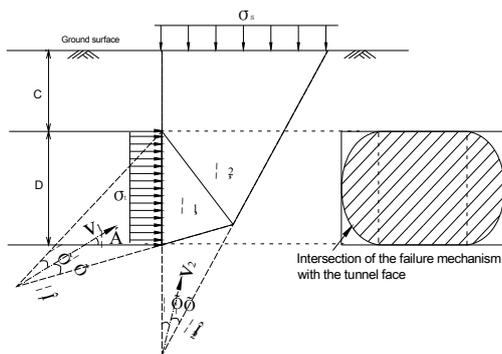
Fig.6. Blow-out mechanism (M2)

M2 is also a translational kinematically admissible failure mechanism, and the velocity field and work equation of M2 is similar to those of M1 (for more details, see 3.2 and 3.3 in this paper).

4.2 Numerical results of M2 (blow-out)

In this section, the values of N_γ^b, N_s^b and the critical failure pressure σ_b for M2 are presented. Contrary to M1, the M2 mechanism is always outcrops, so N_γ^b and N_s^b increase with the increasing of C/D value as shown in Fig. 7 and Fig. 8.

Similar to M1, a characteristic curve for the limit jacking force σ_b is drawn as shown in Fig. 9. Unlike the results of M1, the curve indicates an upper bound, above which blow-out failure will occur. And as the M2 mechanism always outcrops, σ_b and C/D have a positive correlation.
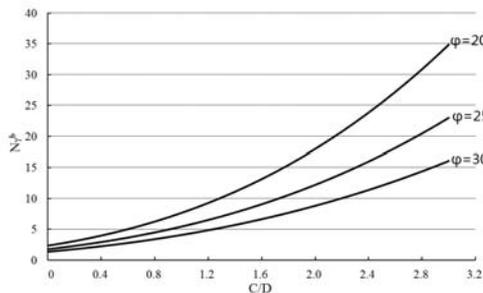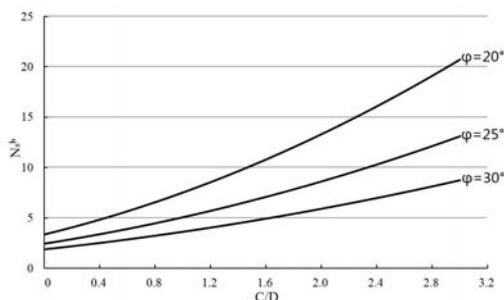

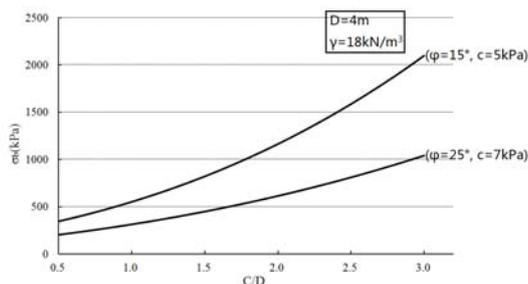Fig.7. Values of N_γ^b

Fig.8. Values of N_s^b

Fig.9. Critical blow-out failure pressure σ_b

5. Conclusions

Two failure mechanisms are presented respectively for collapse failure and blow-out failure, to compute the upper and lower bound of jacking force of a shallow rectangular tunnel for pipe-jacking driven by a pressurized shield. By means of the kinematical approach of limit analysis theory, numerical results of non-dimensional coefficients N_γ and N_s and the limit jacking force σ_t are obtained. Determination of the bound of jacking force is significant to guarantee the tunnel face stability and control the ground subsidence. The conception of cylindrical inserts is imported to solve the modeling problem of the failure surface in rectangular tunnels. It can be extended to the discussion of non-circular tunnels with other forms of cross section in further study.

REFERENCES
[1]   D.N. Chapman, Y. Ichioka. Prediction of jacking forces for microtunnelling operations, Trenchless Technol. Res., 14(1999), NO. 1, 31-41
[2]   K.J. Shou, F.W. Chang. Analysis of pipe-soil interaction for a miniature pipejacking, Journal of Mechanics, 22(2006), NO. 3, 213-220
[3]   Marco Barla, Marco Camusso and Santina Aiassa. Analysis of jacking forces during microtunnelling in limestone, Tunnelling and Underground Space Technology, 21(2006), NO.6, 668-683
[4]   E. Leca, L. Dormieux. Upper and lower bound solutions for the face stability of shallow circular tunnels in frictional material, Géotechnique, 40(1990), NO. 4, 581-606
[5]   D. C. Drucker, W. Prager, and H. J. Greenberg. Soil mechanics and plastic analysis or limit design, Q. Appl. Math, 10(1952), NO. 2, 157-165
[6]   R. L. Michalowski. Limit analysis in stability calculations of reinforced structures, Geotextiles and Geomembranes, 16(1998), NO. 6, 311-331
[7]   R. L. Michalowski, A. Drescher. Three-dimensional stability of slopes and excavations, Géotechnique, 59(2009), NO.10, 839-850
[8]   A.-H. Soubra, D. Dias, F. Emeriault and R. Kastner, Three-dimensional face stability analysis of circular tunnels by a kinematical approach, Geocongress, New Orleans, Louisiana, 2008; 894-901
[9]   R. L. Michalowski. Limit analysis and stability charts for 3D slope failures, Journal of Geotechnical and Geoenvironmental Engineering, 136(2010), NO. 4, 583-593
[10]   W. F. Chen, Limit analysis and soil plasticity. Elsevier, Amsterdam 1975

Authors*: The common address for correspondence of all authors: School of engineering and technology, China University of Geosciences (Beijing), Beijing, 100083, China. Hongan Li, E-mail: lha417@126.com; Yuyou Yang, E-mail: yangyuyou@cugb.edu.cn; Xiaoming Tu, E-mail: xiaomingtu918@163.com;Ting Wang, E-mail: bjcaso@yahoo.com.cn.*